First global study of super dense gluonic matter with UPCs by ALICE

Simone Ragoni[1,*] on behalf of the ALICE Collaboration

[1]Creighton University

Abstract. ALICE was the first experimental collaboration observing a moderate nuclear suppression down to low Bjorken-x in lead nuclei using coherent J/ψ photoproduction. In this contribution, we present new results extending the studies of the photonuclear cross section by covering the Bjorken-x interval of $1.1 \cdot 10^{-5} < x < 3.3 \cdot 10^{-2}$, corresponding to the photon-nuclear energies $17 < W_{\gamma Pb,n} < 920$ GeV. This is achieved by using multiple methods to extract the energy dependence, including new results on the forward neutron emission accompanying the coherent photoproduction process. These new results, combined with ALICE measurements of J/ψ off a proton target, probe the gluonic structure of the lead nuclei at the lowest Bjorken-x possible with any current experiment, challenging both gluon saturation and shadowing models to describe the data.

1 Introduction

Vector meson photoproduction in p–Pb and Pb–Pb ultra-peripheral collisions (UPCs) is actively being studied at the CERN LHC. In these events, a photon from one of the two nuclei interacts with a colourless object from the other nucleus, resulting in the production of a vector meson. J/ψ photoproduction has been studied in ALICE and is sensitive to phenomena such as gluon saturation and nuclear shadowing.

2 ALICE results for J/ψ photoproduction in p–Pb UPCs

The ALICE Collaboration has measured exclusive J/ψ photoproduction in p–Pb UPCs with both Run 1 and Run 2 data. In this particular case, the photon flux is predominantly due to the lead ion, making it possible to unambiguously tag the photon emitter. In this way, the vector-meson rapidity y can be directly related to the Bjorken-x of the collision. ALICE Run 1 and Run 2 data cover the Bjorken-x range $10^{-5} \lesssim x \lesssim 10^{-2}$. From figure 1 [1] it can be seen that the cross sections exhibit a smooth growth from high to low Bjorken-x over the full coverage, which can be described with a power-law fit. This, in turn, indicates that there is no change in the behaviour of the gluon distributions in the proton for the same range.

*e-mail: simone.ragoni@cern.ch

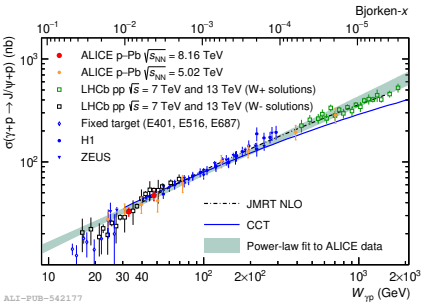

Figure 1. Energy dependence of exclusive J/ψ production in p–Pb ultra-peripheral collisions [1]. The data are described by a power-law growth in the range of Bjorken-x of $10^{-5} \lesssim x \lesssim 10^{-2}$.

3 Measurement techniques for coherent J/ψ photoproduction

The ALICE Collaboration has also measured coherent J/ψ photoproduction in Pb–Pb UPCs, where the term coherent refers to the fact that the photon couples to the entire target nucleus coherently, and hence the vector meson in the final state is characterised by very low transverse momenta of $p_{\mathrm{T}} \lesssim 0.15$ GeV/c. The results obtained by the ALICE Collaboration allow for the extraction of photonuclear cross sections using several techniques, starting from Eq. 1:

$$\frac{\mathrm{d}\sigma_{\mathrm{PbPb}}}{\mathrm{d}y} = n(\gamma, +y) \cdot \sigma_{\gamma\mathrm{Pb}}(+y) + n(\gamma, -y) \cdot \sigma_{\gamma\mathrm{Pb}}(-y)\,, \tag{1}$$

where $\mathrm{d}\sigma_{\mathrm{PbPb}}/\mathrm{d}y$ is the production cross section for coherent J/ψ, $n(\gamma, \pm y)$ are the photon fluxes and $\sigma_{\gamma\mathrm{Pb}}(\pm y)$ are the photonuclear cross sections.

3.1 Coherent J/ψ at midrapidity

At midrapidity, the photon fluxes from the two nuclei are equal because of symmetry. That means that the measured $\mathrm{d}\sigma_{\mathrm{PbPb}}/\mathrm{d}y$ can be directly related to the photonuclear cross section $\sigma_{\gamma\mathrm{Pb}}$ through Eq. 2:

$$\sigma_{\gamma\mathrm{Pb}}(y \sim 0) = \frac{1}{2 \cdot n(\gamma, y \sim 0)} \cdot \frac{\mathrm{d}\sigma_{\mathrm{PbPb}}}{\mathrm{d}y}\,. \tag{2}$$

3.2 Coherent J/ψ at forward rapidity

Eq. 1 can be specialised at forward rapidity, since the photon flux for the low-energy solution is predominant. The photonuclear cross section can then be approximated as shown in Eq. 3:

$$\sigma_{\gamma\mathrm{Pb}}(y) \sim \frac{1}{n(\gamma, y)} \cdot \frac{\mathrm{d}\sigma_{\mathrm{PbPb}}}{\mathrm{d}y}\,. \tag{3}$$

Photonuclear cross sections for both these cases can be extracted from the rapidity dependence of coherent J/ψ as measured by ALICE in [2, 3].

3.3 Measuring coherent J/ψ in peripheral events

At the moment there are two techniques that have been used in ALICE to disentangle the low and high Bjorken-x components. The first one, described in this paragraph, relies on

the measurement of coherent J/ψ in peripheral events. Eq. 1 can also be used for peripheral events, in conjunction with the results in UPCs [4], as shown in Eq. 4:

$$\begin{aligned}\frac{\mathrm{d}\sigma^{\mathrm{P}}_{\mathrm{PbPb}}}{\mathrm{d}y} &= n_{\mathrm{P}}(\gamma,+y)\cdot\sigma_{\gamma\mathrm{Pb}}(+y) + n_{\mathrm{P}}(\gamma,-y)\cdot\sigma_{\gamma\mathrm{Pb}}(-y)\,,\\ \frac{\mathrm{d}\sigma^{\mathrm{U}}_{\mathrm{PbPb}}}{\mathrm{d}y} &= n_{\mathrm{U}}(\gamma,+y)\cdot\sigma_{\gamma\mathrm{Pb}}(+y) + n_{\mathrm{U}}(\gamma,-y)\cdot\sigma_{\gamma\mathrm{Pb}}(-y)\,,\end{aligned} \tag{4}$$

where the symbols P and U indicate peripheral and ultra-peripheral samples, respectively. Thus, a simultaneous fit to both peripheral and UPC results succeeds in disentangling the two solutions.

3.4 Measuring coherent J/ψ in neutron emission classes

The other technique used by ALICE relies on splitting the data set according to neutron emission classes in ultra-peripheral collisions [5]. In this case it is possible to split the two solutions according to Eq. 5 [6]:

$$\begin{aligned}\frac{\mathrm{d}\sigma^{\mathrm{0N0N}}_{\mathrm{PbPb}}}{\mathrm{d}y} &= n_{\mathrm{0N0N}}(\gamma,+y)\cdot\sigma_{\gamma\mathrm{Pb}}(+y) + n_{\mathrm{0N0N}}(\gamma,-y)\cdot\sigma_{\gamma\mathrm{Pb}}(-y)\,,\\ \frac{\mathrm{d}\sigma^{\mathrm{0NXN}}_{\mathrm{PbPb}}}{\mathrm{d}y} &= n_{\mathrm{0NXN}}(\gamma,+y)\cdot\sigma_{\gamma\mathrm{Pb}}(+y) + n_{\mathrm{0NXN}}(\gamma,-y)\cdot\sigma_{\gamma\mathrm{Pb}}(-y)\,,\\ \frac{\mathrm{d}\sigma^{\mathrm{XNXN}}_{\mathrm{PbPb}}}{\mathrm{d}y} &= n_{\mathrm{XNXN}}(\gamma,+y)\cdot\sigma_{\gamma\mathrm{Pb}}(+y) + n_{\mathrm{NXNX}}(\gamma,-y)\cdot\sigma_{\gamma\mathrm{Pb}}(-y)\,,\end{aligned} \tag{5}$$

where 0N0N, 0NXN and XNXN indicate no neutron emission on either sides of the ALICE detector with respect to the interaction point, neutrons only on one side, and neutrons on both sides, respectively.

It is quite interesting to note that different neutron emission classes are characterised by different impact parameter (b) distributions with the following hierarchy: $\langle b\rangle_{\mathrm{0N0N}} > \langle b\rangle_{\mathrm{0NXN}} > \langle b\rangle_{\mathrm{XNXN}}$ [5]. Thus, the two techniques shown in Sect. 3.3 and 3.4 both depend on the impact parameter range, and are complementary to each other.

4 ALICE results in Pb–Pb collisions

The photonuclear cross sections measured by the ALICE Collaboration in Pb–Pb collisions are shown in figure 2(a) [7]. The results obtained with the neutron emission technique are shown by the black points while the blue points in the figure represent those obtained using the technique discussed in Sect. 3.3 using Run 1 results for both peripheral and UPC coherent J/ψ. It is interesting to note that the results with the peripheral technique agree with those obtained with the neutron emission technique. The neutron emission results constitute the first effort to measure nuclear shadowing down to scales of Bjorken-$x \sim 10^{-5}$, thus extending the range in energy by about 300 GeV compared to the peripheral technique. The neutron emission results agree with STARlight [8] at low energies, while at higher energies they agree with models including nuclear shadowing and gluon saturation phenomena.

It is also possible to measure the nuclear suppression factor, which is defined as $S_{\mathrm{Pb}}(x) = \sqrt{\sigma^{\mathrm{data}}_{\gamma\mathrm{Pb}}/\sigma^{\mathrm{IA}}_{\gamma\mathrm{Pb}}}$ [9], where $\sigma^{\mathrm{data}}_{\gamma\mathrm{Pb}}$ is the measured photonuclear cross section, and $\sigma^{\mathrm{IA}}_{\gamma\mathrm{Pb}}$ is the prediction from the Impulse Approximation. Figure 2(b) shows the results obtained for the

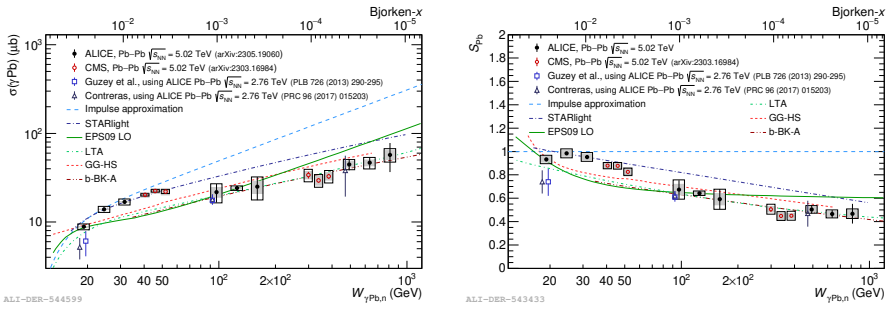

(a) (b)

Figure 2. The energy dependence of the photonuclear cross section and of the nuclear suppression factor are shown in figure 2(a) and 2(b), respectively [7]. $W_{\gamma\mathrm{Pb,n}}$ is the photon–nucleon center of mass energy.

nuclear suppression factor, which shows a decrease from a value of about 0.9 at high Bjorken-$x \sim 10^{-2}$ down to about 0.5 at $x \sim 10^{-5}$, in agreement with models including nuclear shadowing and saturation phenomena. The results from the CMS Collaboration [10] cover the gaps in energy not covered by the ALICE acceptance, thus giving a complete view of the energy dependence of the photonuclear cross sections.

References

[1] S. Acharya *et al.* [ALICE], [arXiv:2304.12403 [nucl-ex]].

[2] S. Acharya *et al.* [ALICE], Phys. Lett. B **798** (2019), 134926 doi:10.1016/j.physletb.2019.134926 [arXiv:1904.06272 [nucl-ex]].

[3] S. Acharya *et al.* [ALICE], Eur. Phys. J. C **81** (2021) no.8, 712 doi:10.1140/epjc/s10052-021-09437-6 [arXiv:2101.04577 [nucl-ex]].

[4] J. G. Contreras, Phys. Rev. C **96** (2017) no.1, 015203 doi:10.1103/PhysRevC.96.015203 [arXiv:1610.03350 [nucl-ex]].

[5] A. J. Baltz, S. R. Klein and J. Nystrand, Phys. Rev. Lett. **89** (2002), 012301 doi:10.1103/PhysRevLett.89.012301 [arXiv:nucl-th/0205031 [nucl-th]].

[6] V. Guzey, M. Strikman and M. Zhalov, Eur. Phys. J. C **74** (2014) no.7, 2942 doi:10.1140/epjc/s10052-014-2942-z [arXiv:1312.6486 [hep-ph]].

[7] S. Acharya *et al.* [ALICE], JHEP **10** (2023), 119 doi:10.1007/JHEP10(2023)119 [arXiv:2305.19060 [nucl-ex]].

[8] S. R. Klein, J. Nystrand, J. Seger, Y. Gorbunov and J. Butterworth, Comput. Phys. Commun. **212** (2017), 258-268 doi:10.1016/j.cpc.2016.10.016 [arXiv:1607.03838 [hep-ph]].

[9] V. Guzey, E. Kryshen, M. Strikman and M. Zhalov, Phys. Lett. B **816** (2021), 136202 doi:10.1016/j.physletb.2021.136202 [arXiv:2008.10891 [hep-ph]].

[10] A. Tumasyan *et al.* [CMS], [arXiv:2303.16984 [nucl-ex]].